

Research article

Effects of filler contacts and interface thermal resistance on the thermal conductivity of heterogeneous spherical filler composites

Yuanyuan Zhang¹, Xiaojian Wang^{1*}, Honghong Li¹, Xinru Fu¹, Simin Huang², Hao Zhou³

¹Department of energy and power engineering, College of Electrical Engineering, Xinjiang University, 830047 Urumqi, China

²Guangdong Provincial Key Laboratory of Distributed Energy Systems, Dongguan University of Technology, 523808 Dongguan, China

³State Key Laboratory of Clean Energy Utilization, Zhejiang University, 310027 Hangzhou, China

Received 4 June 2024; accepted in revised form 6 August 2024

Abstract. Adding heterogeneous fillers with high thermal conductivity (TC) to polymer has been recognized as an effective way to increase the effective thermal conductivity (ETC) of polymer composites. Extensive researches have been conducted on the ETC of composites with heterogeneous fillers. However, the heat transfer enhancement mechanism of heterogeneous fillers remains unknown, and the combined effects of filler size, filler contact, interface thermal resistance (R_c) and other parameters on the ETC have not been explored. In this study, above combined effects are investigated. The results show that the filler contact and R_c are the key factors determining the ETC. The ETC of composite with filler contacts reaches 2.35 at filler content of 25%, which is 11.9% higher than that without filler contacts. The ETC also strongly depends on the R_c (dimensionless form of R_c) ratio (R_{c1}^*/R_{c2}^*) between two fillers, with it becoming asymmetrical when the amount of R_c^* ($R_{c1}^* + R_{c2}^*$) is larger. The ETCs decrease with the increase of R_{c1}^*/R_{c2}^* when the $R_{c1}^*/R_{c2}^* < 1$, while they increase with R_{c1}^*/R_{c2}^* when the $R_{c1}^*/R_{c2}^* > 1$. When $R_{c1}^* + R_{c2}^*$ is a constant, the ETC increases with the competing effects of R_c^* . The models with filler contacts exhibit higher accuracy than other classical models in calculating the ETC across the entire range of filler content.

Keywords: polymer composite, thermal conductivity, heterogeneous filler, filler contact, interface thermal resistance

1. Introduction

With advancements in industrial technology, electronic components are rapidly evolving towards greater integration, miniaturization and higher power. The issue of heat dissipation in fields such as the aerospace industry, electronic devices, chips and energy storage systems is becoming increasingly prominent; this issue significantly affects their performance and service life [1–5]. To address this challenge, the development of high thermal conductive (TC) materials has become an urgent matter. Polymer materials have garnered widespread attention due to their characteristics in lightweight, low cost

and exceptional insulating capabilities [6, 7]. However, most polymers have not been used in the fast heat dissipation of modern electronics due to their extremely low TC ($< 0.4 \text{ W}/(\text{m} \cdot \text{K})$) [8, 9].

The most effective approach to solve this problem is to incorporate high TC fillers into the polymer matrix, the effective thermal conductivity (ETC) of the polymer will be improved effectively [10, 11]. In general, the shapes of these fillers are spheres, ellipsoids, fibers or flakes. Filler shape is a key factor influencing the ETC of composites [12]. Spherical fillers are particularly popular due to their smooth surface and easy dispersion in the polymer matrix,

*Corresponding author, e-mail: xjwang@xju.edu.cn

© BME-PT

and they have become a substitute for other thermal conductive fillers. Composites filled with heterogeneous spherical fillers have a higher ETC than those with only a single filler. The heterogeneous filler refers to differences in size and material. Extensive research has already been conducted on the ETC of composites filled with heterogeneous spherical fillers. Bae *et al.* [13] observed that the ETC of composites achieved 5.2 W/(m·K) by using 2 and 30 μm aluminum nitride (AlN) as fillers for phenolic resin at a small filler content of 20%. This was 1.06 times greater than the composites filled with 30 μm single AlN. Choi and Kim [14] developed two composites, one filled with 10 μm aluminum nitride (AlN) and 0.5 μm aluminum oxide (Al_2O_3), while the other filled with 0.1 μm AlN and 10 μm Al_2O_3 . When the total volume fraction (VF) of fillers reached 58.4%, and the filler content ratio between big and small fillers was 7:3, the ETC of these two composites reached 3.402 and 2.842 W/(m·K). Chen *et al.* [15] indicated that the epoxy/spherical alumina composites achieved the maximum ETC of 1.364 W/(m·K) by adding a mixture 5 μm filler of 20% and 30 μm filler of 80% into the epoxy resin (EP) when the total filler content was 20 vol%, this showed a 531% increase over the pure EP. Ouyang *et al.* [16] reported the composites filled with 75 wt% multi-dimensional network Al_2O_3 exhibited the greatest ETC of 4.01 W/(m·K), which was 18 times as much as the pure polymer. Wang *et al.* [17] discovered that the addition of 5 and 40 μm spherical Al_2O_3 blends to the alumina foam (AF) significantly elevated the ETC of the composites. Once the filler content is 57.6%, there was a drastic enhancement in the ETC of composites, rising from 0.7 to 4.1 W/(m·K), and the corresponding reinforcement increased from 264 to 2097%. Yang *et al.* [18] found that when the volume ratio of 20 μm spherical boron nitride, 70 μm spherical boron nitride and 160 μm spherical boron nitride was 0.224:0.374:0.402, the ETC of the composite is the best. The maximum ETC of the composite is 1.84 W/(m·K), which is 8 times that of pure epoxy resin. Zhou *et al.* [19] filled the silicone rubber (SR) matrix with 30 and 120 μm spherical heterogeneous boron nitride (sBN) fillers. The sBN/SR composites with a filler content of 35% achieved a higher ETC of 1.70 W/(m·K) once the ratio of sBN120 to sBN30 was 8:2, representing an 8.5 times increase compared to pure SR. Li *et al.* [20] showed by experiments that the thermal conductivity of

spherical Al_2O_3 and AlN-filled composites with different particle sizes was higher than that of single-filled composites. Zheng *et al.* [21] added spherical diamond and silver to the epoxy composite exhibiting excellent thermal conductivity (4.65 W/(m·K)) at a filler content of 80 wt%.

As computer technology continues to progress, numerical models have gained increasing popularity in research endeavors. Compared to experimental studies, numerical models have the advantages of a shorter research period, lower cost, and greater universality. Over the past few decades, several classical models have been suggested in calculating the ETC of composites. These include the series and parallel model [22], the Agrawal model [23], the Lewis-Nielsen model [24], the Ngo-Byon model [25], the Hashin-Shtrikman model [26], and others [27]. However, these models primarily focus on studying a single filler and analyzing the impact of its shape, size, and VF of fillers on the ETC. The combined impacts of the filler contacts and the interface thermal resistance (R_c) have not been thoroughly considered in classical models. The heterogeneous fillers are easy to contact each other and form the heat conduction paths, and the heat transfer enhancement effect is obviously higher than that of single size fillers.

This work is to reveal the heat transfer enhancement of heterogeneous spherical fillers on the composite materials, specially focusing on the effect of filler contact, filler size and R_c^* (a dimensionless form of R_c). The coupled effects of filler contact, R_c^* and several other parameters, such as K^* (a dimensionless form of thermal conductivity) and V^* (a dimensionless form of filler size) on the ETC of composites, are extensively revealed by three-dimensional models. Moreover, these numerical models are compared with several classical models to validate their reliability and applicability. This study provides valuable insights and a foundation for improving the ETC of composites.

2. Numerical work

2.1. Generation of cell model

The polymer composite should contain enough fillers for ensure the accuracy of the thermal conduction model, and the distribution of these fillers should accurately reflect its distribution in the actual polymer composite. However, excessive model size results in a rapid increase in computation time and

physical memory. Therefore, a $1 \times 1 \times 1$ cube is used as a three-dimensional cell model in this study, where 1 is the standard size for a dimensionless model. This three-dimensional model contains a large quantity of fillers, representing a periodically repeated cross-section within the polymer composites [28]. The calculation accuracy of this model is much higher than the two-dimensional model. The filler shape is spherical, and its size is different. This cell model is generated by Gambit software, a commonly used commercial software for generating physical models.

Figure 1 illustrates the positions of small and large fillers in the polymer matrix. An in-house computational program has been devised to generate the spatial locations of the fillers. The process stops once the desired content is achieved. For large fillers [29], the center position can be represented by the coordinate points (x_1, y_1, z_1) . The dimensions of the cell model are labelled L_x , L_y and L_z , respectively. The computer program generates random numbers r_x , r_y and r_z , ranging from 0 to 1. These random numbers satisfy a uniform distribution. The coordinate of x_1 is calculated by multiplying r_x with L_x . Similarly, the coordinates of y_1 and z_1 are obtained by multiplying their respective corresponding factors. The coordinates of small spherical fillers are generated by a similar manner. The computer-generating process of heterogeneous filler position is basically the same as the mixed forming process of heterogeneous fillers and polymer matrix in polymer composite. The dis-

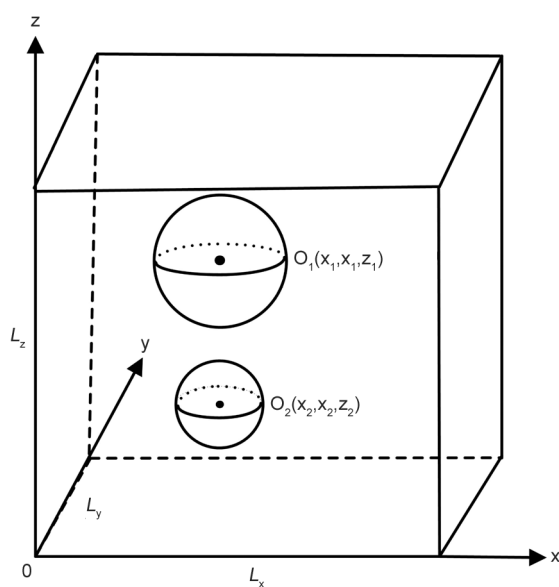


Figure 1. Schematic of a big filler and a small filler in polymer matrix.

tribution of heterogeneous fillers in this numerical model can reflect the real distribution of heterogeneous fillers in the polymer composite. Eight three-dimensional models are generated for each filler content, and the effective thermal conductivity of the polymer composite is the average value of the calculated thermal conductivity of the eight models. The standard deviation of thermal conductivity calculated by eight models is less than 8%.

Figure 2 displays the three-dimensional model utilized for numerical calculations and its corresponding boundary conditions. This model contains numerous large spherical fillers (filler-1) and small spherical fillers (filler-2). The distribution of heterogeneous fillers exhibits considerable randomness, accompanied by filler contacts. Filler contact is the most important factor to improve the thermal conductivity of polymer composite. The larger filler and thermal conductive networks are formed by the filler contact, which is the key to greatly improving the thermal conductivity of the polymer material. The filler contacts exist in the actual polymer composite and increase with the increase of filler content. This model is closer to the actual polymer composite and has higher accuracy in predicting the thermal conductivity of polymer composite.

The side walls of this cell model are the adiabatic boundaries, while its upper and lower walls are isothermal boundaries. The thermal conductivities of all heterogeneous spherical fillers and polymer matrix are constants. Boundary conditions do not affect the heat transfer in the numerical models. These are used for the convenience of the numerical calculation.

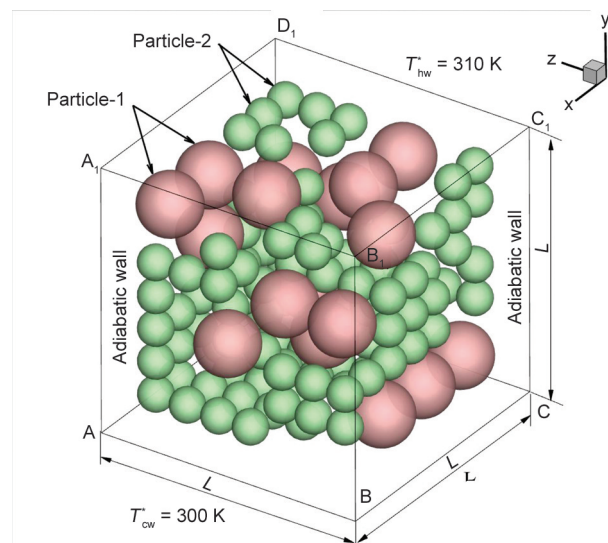


Figure 2. Three-dimensional numerical model and boundary conditions.

L represents the size of the cell model, T_{hw} denotes the temperature of the hot side, whereas T_{cw} signifies the temperature of the cold side.

2.2. Numerical calculation

The heat transfer mechanism in composite adheres to Fourier's law, and its characteristics can be described through Laplace's equation. This is the three-dimensional governing equation (Equation (1)):

$$\frac{\partial}{\partial x} \left(\frac{\partial T_i}{\partial x} \right) + \frac{\partial}{\partial y} \left(\frac{\partial T_i}{\partial y} \right) + \frac{\partial}{\partial z} \left(\frac{\partial T_i}{\partial z} \right) = 0 \quad \begin{cases} i = f, m \\ f = f_1, f_2 \end{cases} \quad (1)$$

Filler-1, filler-2 and matrix are indicated by the subscripts “ f_1 ”, “ f_2 ”, and “ m ”.

For solving the governing equations in Equation (1), the parameters x , y , z and T are introduced, which can have no-dimension form as Equation (2):

$$x^* = \frac{x}{L}; \quad y^* = \frac{y}{L}; \quad z^* = \frac{z}{L}; \quad T_i^* = \frac{T_i - T_{cw}}{T_{hw} - T_{cw}}; \quad (2)$$

where L represents the characteristic length, which is also equivalent to the dimension of this model, as is showed in Figure 2. Therefore, Equation (2) is used to non-dimensionalize the governing equation from Equation (1) as Equation (3):

$$\frac{\partial}{\partial x^*} \left(\frac{\partial T_i^*}{\partial x^*} \right) + \frac{\partial}{\partial y^*} \left(\frac{\partial T_i^*}{\partial y^*} \right) + \frac{\partial}{\partial z^*} \left(\frac{\partial T_i^*}{\partial z^*} \right) = 0 \quad \begin{cases} i = f, m \\ f = f_1, f_2 \end{cases} \quad (3)$$

The boundary conditions are depicted in Figure 2. All side walls are adiabatic, while the top and bottom walls are isothermal. This means that the inlet and outlet temperatures can be adjusted, and the heat flow predominantly occurs along the z -axis direction. This study extensively examines the effect of interface thermal resistance (R_c). It is treated as a virtual interface layer, which has constant thickness (d_{il}) and thermal conductivity (k_{il}). The interface between the two materials is subject to the following specific boundary conditions Equation (4) [30]:

$$\begin{cases} -n_m \cdot \nabla T_m^* = -\frac{T_f^* - T_m^*}{R_c^*} \\ -n_f \cdot (\kappa \nabla T_f^*) = -\frac{T_m^* - T_f^*}{R_c^*} \end{cases} \quad (4)$$

The TC of filler to that of matrix material is denoted by κ . The dimensionless definition of R_c is given as Equation (5):

$$R_c^* = R_c \frac{K_m}{L} = \frac{d_{il}^*}{k_{il}^*} \quad (5)$$

where k_{il}^* is the mean harmonic average TC of the heterogeneous filler and the polymer matrix. Consistent with Tsekmes' hypothesis, this definition indicates that the TC value at the interface is slightly higher than that the TC of the polymer matrix [31]. The thickness (d_{il}^*) of the virtual interface layer is determined by the contact conditions between the filler and the polymer matrix.

The thickness of the interface will be normalized based on the characteristic length, and the d_{il}^* and k_{il}^* which are no-dimension parameters in Equation (5) can be defined as Equation (6):

$$d_{il}^* = \frac{d_{il}}{L}; \quad k_{il}^* = \frac{k_{il}}{L} = \frac{2\kappa}{\kappa + 1}; \quad \kappa = \frac{K_f}{K_m} \quad (6)$$

Additionally, other important dimensionless parameters such as K_1^* , K_2^* , V_1^* and V_2^* are defined as Equation (7):

$$K_1^* = \frac{K_{f1}}{K_m}; \quad K_2^* = \frac{K_{f2}}{K_m}; \quad V_1^* = \frac{V_{sf1}}{K_{model}}; \quad V_2^* = \frac{V_{sf2}}{K_{model}} \quad (7)$$

where K_{f1} , K_{f2} and K_m represent the TC of filler-1, filler-2 and matrix material. V_{sf1} and V_{sf2} represent the volume of single filler-1 and single filler-2. V_{model} is the volume of the entire cell model.

By analyzing the temperature distribution of this numerical model, the ETC of composites is defined by Equation (8):

$$k_{eff} = \frac{Q}{L(T_{hw} - T_{cw})} \quad (8)$$

where Q is the total heat flux through the cell model, which can be calculated by integrating the heat flux over the upper or lower surface. It has basically the same value on the upper surface and the lower surface, with a maximum deviation of no more than 1%, and its effect on the result is negligible. Equation (8) can be written as (Equation 9):

$$k_{eff}^* = \frac{k_{eff}}{K_m} \quad (9)$$

Equations (1)–(9) for coupling heat conduction in the polymer matrix, heterogeneous fillers and virtual interface layer are solved by finite difference technique. The cell model is discretized by finite volume

method (FVM). The discretized equations are solved by central difference scheme. A validated commercial software (FLUENT) is used in the analysis to calculate temperature fields. When the heat flux on the z direction is known, the effective thermal conductivity is calculated by Equation (8) and Equation (9). The desktop computer is performed for these numerical simulations.

2.3. Grid processing

Grid processing plays a crucial role in the numerical calculation of heat conduction models. Grid density is a crucial factor that significantly impacts the reliability of computational results. The grid independence test has been performed to guarantee the accuracy of the numerical analysis. The filler shape is spherical, and $V_2^* = 6V_1^* = 0.006$, $K_1^* = K_2^* = 1000$, $R_{c1}^* = R_{c2}^* = 0.05$. R_c^* is the dimensionless form of R_c . Table 1 presents the computed outcomes along with the corresponding time taken for k_{eff}^* of composites with different grid densities. k_{eff}^* is the dimensionless

Table 1. k_{eff}^* and time consumptions with different grid densities. ($V_2^* = 6V_1^* = 0.006$, $K_1^* = K_2^* = 1000$, $R_{c1}^* = R_{c2}^* = 0.05$).

Grid number	Meshing time [s]	Calculation time [min]	Relative thermal conductivity
15 625	985	895	2.211
125 000	1987	1963	2.113
1000 000	4172	3758	2.085

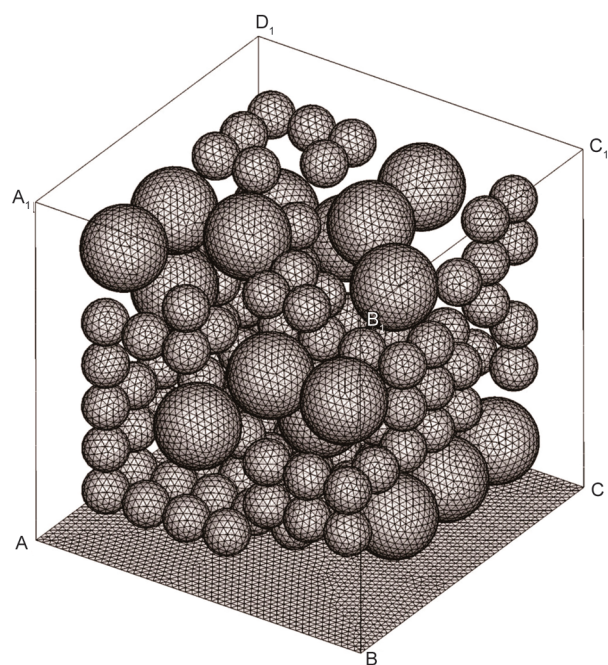


Figure 3. The grid structure of a cell model (only showing the bottom surface and fillers).

form of thermal conductivity of polymer composites (k_{eff}). It is observed that the relative TC of composites exhibits negligible changes when the grid density exceeds $50 \times 50 \times 50$ ($1.25 \cdot 10^5$). However, the time required for meshing and numerical calculation significantly increases with grid density. The difference in relative thermal conductivity caused by grids of $50 \times 50 \times 50$ ($1.25 \cdot 10^5$) and $100 \times 100 \times 100$ (10^6) is no more than 2%. Consequently, a grid number of $50 \times 50 \times 50$ ($1.25 \cdot 10^5$) is chosen for the numerical calculations in this study. This choice not only saves a significant amount of time but also improves the computational efficiency. Figure 3 displays the schematic of the computing grid. For improving the visualization of fillers, only the bottom grid of the model is exhibited.

3. Results and discussion

3.1. Competing effects of heterogeneous filler

Interface properties, particularly R_c^* , have a vital function in determining heat transfer characteristics of composites. The roughness of contact surfaces between distinct phases constitutes this property, exerting a considerable influence on the ETC [32, 33]. This section focuses on examining the effect of R_c^* on the ETC of composites when the filler is in contact.

Figure 4 illustrates the conflicting effects of heterogeneous filler on R_c in three different scenarios of filler volume fraction: $V_1^* < V_2^*$ (Figure 4a); $V_1^* = V_2^*$ (Figure 4b); and $V_1^* > V_2^*$ (Figure 4c). In all cases, the $V_1^* + V_2^*$ is a fixed value. This figure contains 5 curves, each of which is connected by 11 points. When filler-1 is not in contact with filler-2, R_{c1}^* and R_{c2}^* independently effect the ETC. However, a large filler will be formed by filler contact between filler-1 and filler-2, and the effect of the large filler on the ETC is realized jointly by R_{c1}^* and R_{c2}^* . The values of R_{c1}^* and R_{c2}^* can be easily solved by $R_{c1}^* + R_{c2}^*$ and R_{c1}^*/R_{c2}^* . $R_{c1}^* + R_{c2}^*$ and R_{c1}^*/R_{c2}^* can reflect the synergistic effect of filler-1 and filler-2 on the ETC.

It is important to note that the TCs of the heterogeneous filler are kept constant for these cases, with low K_1^* ($= 2$) and high K_2^* ($= 500$) being used as examples. Consequently, while the $R_{c1}^* + R_{c2}^*$ is very small, the ETC curves exhibit symmetry with respect to the vertical line $R_{c1}^*/R_{c2}^* = 1$. This is shown by the lines $R_{c1}^* + R_{c2}^* = 10^{-4}$ and $R_{c1}^* + R_{c2}^* = 0.01$ in Figure 4. However, when the $R_{c1}^* + R_{c2}^*$ is large, the ETC becomes highly dependent on the R_c^* ratio and

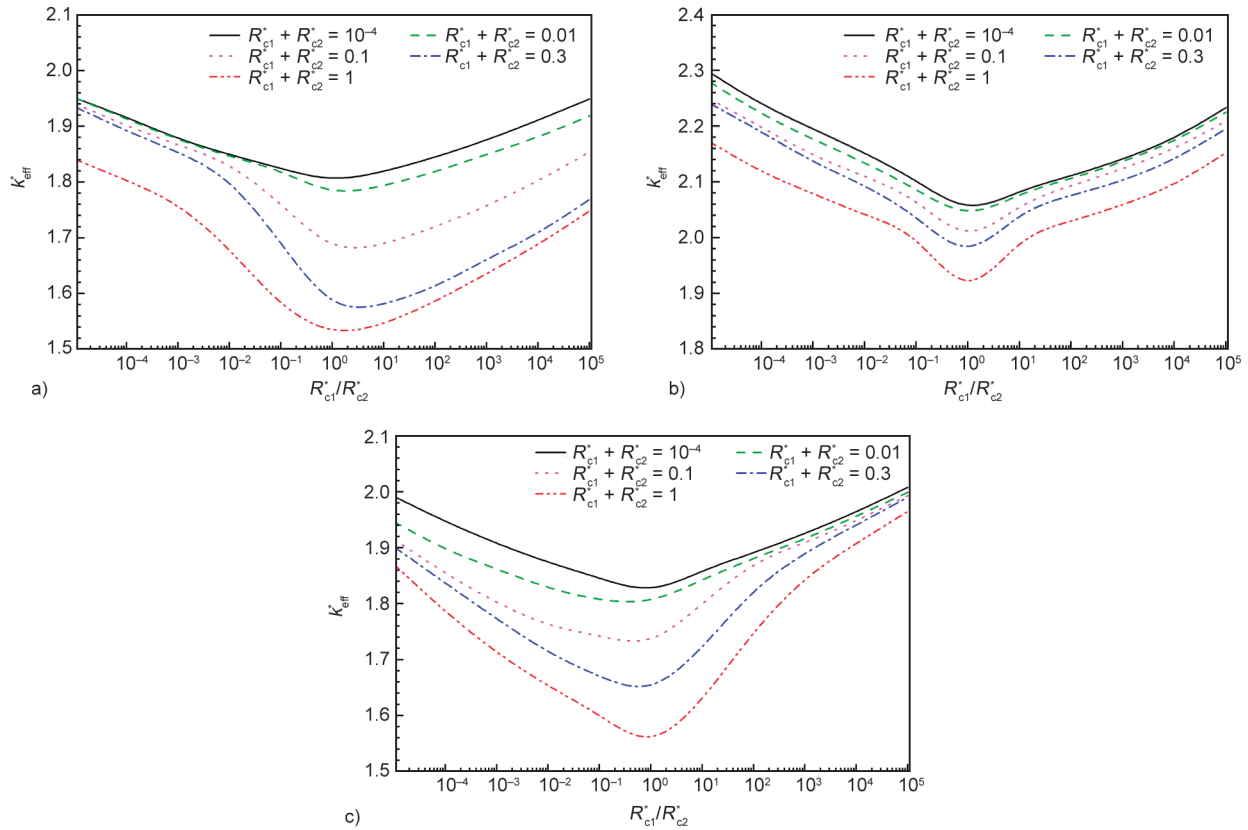


Figure 4. Competing effects of heterogeneous filler in terms of the R^* and filler size: $K_1^* = 2$, $K_2^* = 500$, a) $V_1^* = V_2^*/6 = 0.001$, b) $V_1^* = V_2^* = 0.003$, c) $V_1^* = 6V_2^* = 0.006$.

exhibits asymmetrical. That is indicated by the lines of $R_{c1}^* + R_{c2}^*$ corresponding to 0.1, 0.3 and 1 in Figure 4. Furthermore, visually examining the figure reveals that the variation of the curves can be roughly divided into two parts. Once the R_{c1}^*/R_{c2}^* is between 0 and 1, all the ETC curves decrease, and their slopes are negative as R_{c1}^*/R_{c2}^* increases, regardless of the change in the $R_{c1}^* + R_{c2}^*$. Moreover, this trend abruptly reverses if the R_{c1}^*/R_{c2}^* is between 1 and 10^5 . In this range, all the ETC curves steadily increase with positive slopes. These results indicate that the variation in ETC of composites is determined by the dominant position R_c^* between the two fillers. The decrease in the curve is dominated by an increase of R_{c1}^* while the increase in the curve is mainly influenced by a decrease of R_{c2}^* . The ETC of composites is also influenced by the $R_{c1}^* + R_{c2}^*$. While the $R_{c1}^* + R_{c2}^*$ is no more than 0.01, the minimum ETC values are obtained on the vertical line $R_{c1}^*/R_{c2}^* = 1$. However, as the $R_{c1}^* + R_{c2}^*$ exceeds 0.01, they move to the right of the line $R_{c1}^*/R_{c2}^* = 1$ with the increase of R_{c1}^*/R_{c2}^* .

Figure 4a represents large fillers with a high TC, Figure 4b shows fillers of the same size but with different TC, and Figure 4c represents the competing

effects of the R_c^* of the composites with heterogeneous fillers on their ETC when the TC of large fillers is low. The difference in ETC caused by filler size is significant when $K_1^* < K_2^*$ is fixed. By comparing the obtained ETC values under the three conditions: $V_1^* < V_2^*$, $V_1^* = V_2^*$ and $V_1^* > V_2^*$, the effects of fillers can be observed. Comparing Figure 4a with Figure 4c, it is found that the ETC values are 1.06 times higher at $V_1^* < V_2^*$ compared to $V_1^* > V_2^*$. This demonstrated that large fillers with lower TC pose challenges in improving the ETC of composites when $K_1^* + K_2^*$ is a fixed value. In other words, when the TC of the small filler is the same as that of the matrix material (which means the TC at large filler approach $K_1^* + K_2^*$), it becomes easier to enhance the ETC of composites. This provides guidance for increasing the ETC of composites by increasing the TC of large fillers when the $K_1^* + K_2^*$ is a fixed value. Furthermore, when the competing effects of R_c^* are similar, the ETC of composites with homogeneous or heterogeneous heterogeneous fillers significantly depends on the synergistic effects of V^* and K^* of fillers. The ETC of polymer composites filled with heterogeneous fillers is affected by various physical parameters. The interface thermal resistance is small.

The heat flow into the composite material can be relatively easy to collect in the upper part of the filler. The accumulation rate of heat flow in the upper part of the filler, the outflow rate of heat flow in the lower part of the filler and the overall enhanced heat transfer of the filler all decrease with the increase of the interface thermal resistance. Under the same filler content, the heat transfer path of the large filler is longer, which reduces the number of heat flow through the interface layer, and then improves the thermal conductivity of the polymer composite. The decrease of interfacial thermal resistance of large fillers is more conducive to the improvement of thermal conductivity than that of small fillers.

Figure 5 demonstrates the competing impacts of heterogeneous fillers on the R_c^* and TC of two fillers, with the V^* remaining constant. The figure considers three specific cases of TC: $K_1^* < K_2^*$ (Figure 5a), $K_1^* = K_2^*$ (Figure 5b), and $K_1^* > K_2^*$ (Figure 5c). Like Figure 4, the ETC curves on the left of $R_{c1}^*/R_{c2}^* = 1$ have negative slopes, while those on the right have positive slopes. This implies that the competing effects of R_c^* for two fillers increase, the ETC of the composites also increases at a given $R_{c1}^* + R_{c2}^*$.

The ETC curves are symmetric with respect to the line of $R_{c1}^*/R_{c2}^* = 1$ while $K_1^* = K_2^*$, and the minimum ETC line coincides exactly with the vertical axis $R_{c1}^*/R_{c2}^* = 1$. However, it becomes asymmetrical once $K_1^* \neq K_2^*$. In the case of $K_1^* > K_2^*$ (Figure 5c), the ETC values on the right side of the vertical line ($R_{c1}^*/R_{c2}^* = 1$) are slightly bigger than those on the left. The trend is suddenly reversed when $K_1^* \leq K_2^*$, as shown in Figure 5a and Figure 5b. To get a higher ETC, R_{c1}^* could be smaller than R_{c2}^* while K_1^* exceeds K_2^* , and vice versa.

It should be noted that the ETC is the highest when $K_1^* = K_2^*$, while it is the lowest when $K_1^* < K_2^*$, for a given case of $V_1^* < V_2^*$ and the R_c^* kept constant. The ETC of composites with fillers $K_1^* = K_2^*$ is 1.2 times higher than that of $K_1^* \neq K_2^*$. This indicates that composites with heterogeneous fillers of the same materials have better thermally conductive performance. The larger the TC of two fillers, the greater the ETC of composites. Therefore, the TCs of heterogeneous fillers should be equal and large enough, which is the key to obtain higher ETC. When the total thermal resistance is constant ($R_{c1}^* + R_{c2}^*$), the ETC of the polymer composite is the worst when the interfacial

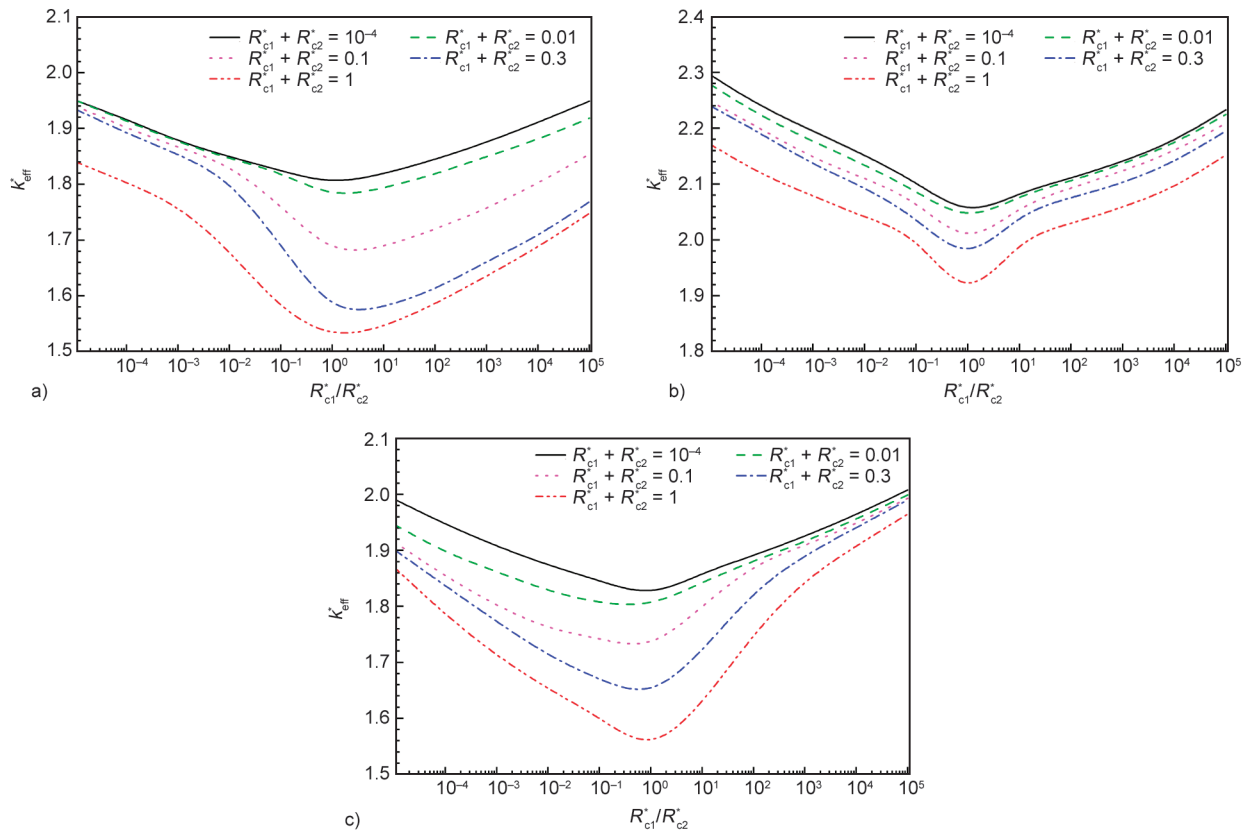


Figure 5. Competing effects of heterogeneous filler in terms of the R^* and K^* : $V_2^* = 2V_1^* = 0.006$, a) $K_1^* = 2, K_2^* = 500$; b) $K_1^* = 251, K_2^* = 251$; c) $K_1^* = 500, K_2^* = 2$.

thermal resistance is equally distributed ($R_{c1}^*/R_{c2}^* = 1$). In general, the heat transfer capacity of the filler is much greater than that of the polymer matrix, and the heat is easy to gather around the filler. The interfacial thermal resistance reduces the comprehensive heat transfer performance of the filler. The overall heat transfer effect of multiple general heat transfer channels (fillers) is lower than that of one excellent heat transfer channel (filler). In the case of a certain filler size and filler contact, it is better to replace the filler with a good thermal conductivity than to increase the filler content.

3.2. Effects of filler thermal conductivity

Figure 6 shows that the ETC varies with the TC of filler-1 for different TCs of filler-2 in four specified cases of R_c^* : $R_{c1}^*/R_{c2}^* = 0$ (Figure 6a), $R_{c1}^*/R_{c2}^*/5 = 0.01$ (Figure 6b), $R_{c1}^*/R_{c2}^* = 0.05$ (Figure 6c), and $R_{c1}^*/R_{c2}^* = 0.25$ (Figure 6d). It can be observed that the single filler (filler-1) effectively increases the ETC of composites while the TC of filler-2 is assumed to be a constant value ($K_2^* = 1$), as indicated by the solid lines in Figure 6. Additionally, it was found that the ETC consistently increases with increases of

K_2^* for all fixed values of K_1^* . However, as the K_1^* increases, the ETC increases sharply. When K_1^* approaches its critical value of approximately 10^3 , the growth rate of ETC gradually slows down until it reaches a steady state. Beyond this threshold value, the ETC does not increase with the increase of K_1^* and becomes a function of K_2^* . Therefore, the ETC of composites significantly depends on the synergistic effects between the TCs of two fillers.

Additionally, as depicted in the figure, the ETC decreases with an increase of R_c^* , regardless of the variations of TC between two fillers. When K_1^* reaches 10^3 , the ETC at $R_{c1}^* = R_{c2}^* = 0$ is 1.17 times higher than that at $R_{c1}^* = 5R_{c2}^* = 0.25$ for a line where K_2^* equals 1. There exists a clear negative correlation between ETC and R_c^* , with the correlation becoming more evident as the increase of R_c^* . Consequently, those heterogeneous fillers with large R_c^* are not suitable as high thermally conductive fillers to increase the ETC in the matrix. They should be avoided during the production of composites. When the thermal conductivity of the filler is much higher than that of the polymer matrix, the heat transfer in the filler has little resistance compared with the polymer matrix,

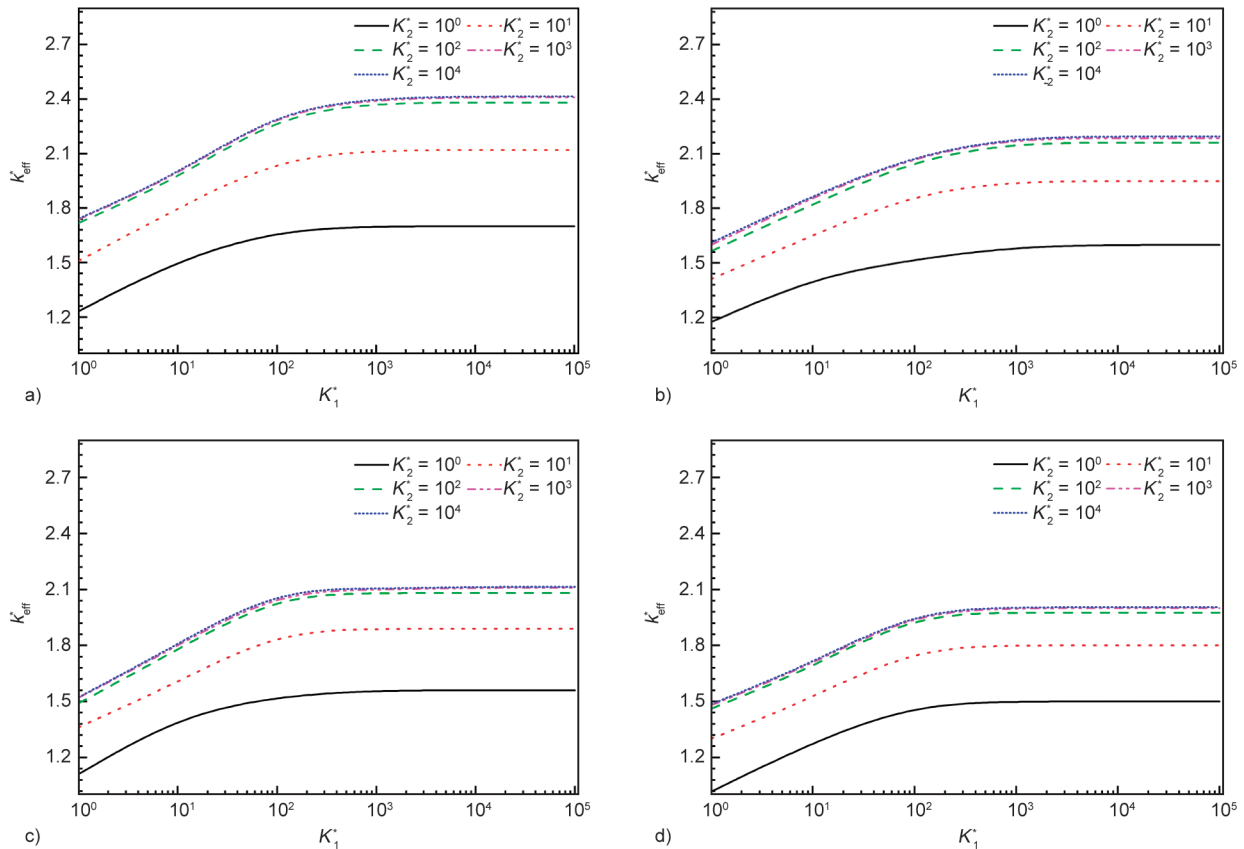


Figure 6. k_{eff}^* as a function of K_1^* and K_2^* , $V_2^* = 6V_1^* = 0.006$, a) $R_{c2}^* = R_{c1}^* = 0$, b) $R_{c2}^* = R_{c1}^*/5 = 0.01$, c) $R_{c2}^* = R_{c1}^* = 0.05$, d) $R_{c2}^* = R_{c1}^* = 0.25$.

which is like superconducting transfer. In this case, the thermal conductivity of the filler is continuously increased, and the thermal conductivity of the composite material is almost not improved.

3.3. Model validation

Figure 7 compares the ETC values obtained from the present numerical models, validated experiments and classical models. In this validated experiment, the filler-1 is alumina oxide with mean particle size of 10 μm , the filler-2 is aluminum nitride with a particle size of 60 μm , and polyethylene is the polymer matrix. The TC of filler-1, filler-2 and epoxy is 22, 195 and 0.23 W/(m·K). The densities of alumina oxide, aluminum nitride and polyethylene are 3.98, 3.25 and 0.94 g/cm³, respectively. The total volume content of filler increases from 0 to 25%. The content ratio of alumina oxide and aluminum nitride is 1:1. Firstly, the heterogeneous filler and polyethylene powder are thoroughly stirred, and then the mixture is hot-pressed to make the polymer composite. The ETC of composite material is measured by Hot Disk (TPS-2500S) at the temperature of 25 °C. Several parameters are set in the numerical analysis and classical models: $K_1^* = 95.7$, $K_2^* = 847.8$, $V_2^* = 6V_1^*$, $\phi_1 = \phi_2$, $R_{c1}^* = R_{c2}^* = 10^{-4}$. Most of the existing classical models do not consider the effect of interface thermal resistance. To be consistent with these classical models, set $R_{c1}^* = R_{c2}^* = 10^{-4}$. When the $R_{c1}^* = R_{c2}^* = 10^{-4}$, the effect of R_c^* on the ETC of polymer composites can be ignored. The effect of interface thermal resistance is not considered in most classical models. The R_c^* is determined by the physical properties and interfacial contact of the filler and polymer matrix. It may also have the same value in

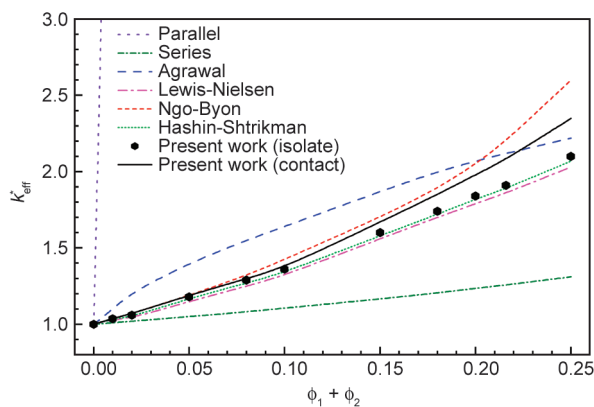


Figure 7. Comparison of numerical models with other models and validated experiment. $K_1^* = 22$, $K_2^* = 195$; $\phi_1 = \phi_2$; $V_2^* = 6V_1^*$; $R_{c2}^* = R_{c1}^* = 10^{-4}$.

the case of different filler sizes and materials. The isolate model refers to a numerical model without filler contact, while a Contact model refers to a numerical model with filler contact. In this paper, two kinds of numerical models are established to study the effect of filler contact on the ETC.

The parallel and series models establish the upper and lower limits of ETC values across all models. The experimental results have highest consistency with the Isolate model, Contact model, Ngo-Byon model, Hashin-Shtrikman model and Lewis-Nielsen model at very low filler content (<5%). Consequently, most models are capable of precisely predicting the ETC of composites with low filler content. At very low filler content, the number and size of large fillers are small, resulting in a negligible effect of filler contact. When the filler volume fraction between 5 and 10%, the ETC curves from the Isolate model, Contact model, Hashin-Shtrikman model and Lewis-Nielsen model match well with those from the validated experiment. As the filler content exceeds 10%, only the Contact model shows good agreement with the experimental results. In these classical models and Isolate models, filler contact on the ETC has yet to be considered. Only the contact model has good applicability and high accuracy under the high filler content.

Another finding is that upon exceeding a 10% filler content, the results which are from the contact model exhibit a slight increase compared to those derived from the isolate model. Particularly, at the filler content of 25%, the Contact model has a high ETC of 2.35, which is 11.9% greater than the ETC obtained from the Isolate model. The effect of filler contact becomes particularly obvious when predicting the ETC of composites with high filler content. Therefore, the filler contact facilitates the formation of heat transfer pathways that are more efficient and enhances the ETC of composites. Hence, the effect of filler contact can not be ignored. Only the Contact model considers the combined effects of filler contact and R_c^* , and it serves as a predictive tool for estimating the ETC of composites filled with high filler content.

4. Conclusions

Using spherical heterogeneous fillers with different sizes significantly enhances the ETC of composites, thanks to the heat conduction pathways provided by filler contacts. Although previous research has been

conducted on the ETC of composites filled with heterogeneous spherical fillers, there is still uncertainty in relation to the combined impact of R_c^* and filler contact on the ETC of composite. This study investigates these effects by three-dimensional numerical models, classical models and validated experiments. The subsequent conclusions can be formulated:

- (1) The ETC curves are symmetric with the line $R_{c1}^*/R_{c2}^* = 1$ while the $R_{c1}^* + R_{c2}^*$ is no more than 0.01. However, the ETC is largely influenced by the R_c^* ratio (R_{c1}^*/R_{c2}^*). Specifically, once the value of $R_{c1}^* + R_{c2}^*$ exceeds 0.01, ETC exhibits asymmetry. The greater the competing effects of heterogeneous filler R_c^* , the better the ETC of composites.
- (2) The ETC of composites filled with spherical heterogeneous fillers can be effectively improved by increasing the filler contacts. At a filler content of 25%, the Contact model achieves a high ETC of 2.35. It is 11.9% higher than that from the Isolate model.
- (3) When $V_1^* < V_2^*$ and $K_1^* + K_2^*$ is a fixed, the maximum ETC values are obtained at $K_1^* = K_2^* = 251$, while the minimum ETC exists under the condition of $K_1^* = 2$, $K_2^* = 251$. The composite with the same material heterogeneous fillers has better thermally conductive performance. The ETC increases with TC of two fillers, either K_1^* or K_2^* . When the TC of filler-1 exceeds a threshold value of 10^3 , the ETC does not increase with increasing the K_1^* and becomes a function of K_2^* .
- (4) Contact models consider the synergistic effect of filler contact, K_1^* , K_2^* , V_1^* , V_2^* , R_{c1}^* and R_{c2}^* on the ETC of composites. These models exhibit greater precision than other classical models in calculating the ETC of composites with heterogeneous fillers across the entire range of filler content.

The research results of this paper can be used to guide the selection of heterogeneous high thermal constructive fillers, the construction of thermal conductive networks, and the optimization of the interface between heterogeneous fillers and polymer matrix. Future research should focus on the high filler content, non-spherical filler and three or more fillers.

Acknowledgements

This work is sponsored by Natural Science Foundation of Xinjiang Uygur Autonomous Region (No. 2022D01C420), Major Science and Technology Projects of Xinjiang Uygur Autonomous Region (No. 2023A01005-2), Tianchi Talents Introduction Plan of Xinjiang Uygur Autonomous Region, State Key Laboratory of Clean Energy Utilization Open Fund Project (No. ZJUCEU2023020) and Guangdong Provincial University Innovation Team Project (No. 2023KCXTD038).

Nomenclature

d_{tl}	interface thickness [m]
L	length of unit cell [m]
K/k	thermal conductivity [W/(m·K)]
V	filler size
T	temperature [K]
Q	overall heat flux [W/m ²]
R_c	interface thermal resistance [s ³ ·K/kg]
x	coordinate of the x -axis [m]
y	coordinate of the y -axis [m]
z	coordinate of the z -axis [m]
n	interface normal [m ⁻¹]

Greek symbols

κ	thermal conductivity ratio of filler and matrix
ϕ	volume fraction

Subscripts, superscripts

hw	hot side
cw	cold side
eff	effective
f	filler
m	polymer matrix
sf	single filler
*	non-dimensional form

References

- [1] Mokoena T. E., Magagula S. I., Mochane M. J., Mokhena T. C.: Mechanical properties, thermal conductivity, and modeling of boron nitride-based polymer composites: A review. *Express Polymer Letters*, **15**, 1148–1173 (2021).
<https://doi.org/10.3144/expresspolymlett.2021.93>
- [2] Yang G., Yang B., Chen X., Wang S., Li C., Liu G., Wu J.: Aluminum micropillar wicks integrated with boehmite nanostructures for rapid heat dissipation. *International Journal of Heat and Mass Transfer*, **223**, 125211 (2024).
<https://doi.org/10.1016/j.ijheatmasstransfer.2024.125211>

- [3] Rajasekaran B., Kumaresan G., Arulprakasajothi M., Vellaiyan S.: Latent heat energy storage using nanomaterials as a heat sink for the prevention of thermal runaway: A study in conjugate heat dissipation. *International Communications in Heat and Mass Transfer*, **151**, 107225 (2024).
<https://doi.org/10.1016/j.icheatmasstransfer.2023.107225>
- [4] Hu J., Geng T., Wang K., Fan Y., Min C., Su H.: Mechanisms for improving fin heat dissipation through the oscillatory airflow induced by vibrating blades. *International Journal of Heat and Mass Transfer*, **220**, 124965 (2024).
<https://doi.org/10.1016/j.ijheatmasstransfer.2023.124965>
- [5] Zhang Y., Liu Y., Qu M., Yao Q., Fu C., Yin S.: Optimization analysis of heat dissipation performance of microchannel heat sinks with the addition of columnar inserts of spiral distribution. *International Journal of Thermal Sciences*, **195**, 108633 (2024).
<https://doi.org/10.1016/j.ijthermalsci.2023.108633>
- [6] Sharma P. K., Chung J-Y.: Poly-flex-antennas: Application of polymer substrates in flexible antennas. *Express Polymer Letters*, **18**, 371–390 (2024).
<https://doi.org/10.3144/expresspolymlett.2024.28>
- [7] Salleh M. S., Ain M. F., Ahmad Z., Abidin I. S. Z., Isa C. M. N. C.: Development of stretchable and bendable polymer wearable antenna for 5G applications. *Express Polymer Letters*, **16**, 1267–1279 (2022).
<https://doi.org/10.3144/expresspolymlett.2022.92>
- [8] Hein L. L., Morteau M. V. V.: Theoretical and experimental thermal performance analysis of an additively manufactured polymer compact heat exchanger. *International Communications in Heat and Mass Transfer*, **124**, 105237 (2021).
<https://doi.org/10.1016/j.icheatmasstransfer.2021.105237>
- [9] Wang H., Guo L., Wang D., Xu B., Chu W., Xu W.: Measuring in-plane thermal conductivity of polymers using a membrane-based modified Ångström method. *International Journal of Thermal Sciences*, **179**, 107701 (2022).
<https://doi.org/10.1016/j.ijthermalsci.2022.107701>
- [10] Qin T. F., Wang H., He J., Qu Q. Q., Da Y. S., Tian X. Y.: Amino multi-walled carbon nanotubes further improve the thermal conductivity of boron nitride/liquid crystal epoxy resin composites. *Express Polymer Letters*, **14**, 1169–1179 (2020).
<https://doi.org/10.3144/expresspolymlett.2020.95>
- [11] Sadej M., Gojzewski H., Gajewski P., Vancso G. J., Andrzejewska E.: Photocurable acrylate-based composites with enhanced thermal conductivity containing boron and silicon nitrides. *Express Polymer Letters*, **12**, 790–807 (2018).
<https://doi.org/10.3144/expresspolymlett.2018.68>
- [12] Wang S., Wen B.: Effect of functional filler morphology on the crystallization behavior and thermal conductivity of PET resin: A comparative study of three different shapes of BN as heterogeneous nucleating agents. *Composites Science and Technology*, **222**, 109346 (2022).
<https://doi.org/10.1016/j.compscitech.2022.109346>
- [13] Bae J-W., Kim W., Cho S-H., Lee S-H.: The properties of AlN-filled epoxy molding compounds by the effects of filler size distribution. *Journal of Materials Science*, **35**, 5907–5913 (2000).
<https://doi.org/10.1023/A:1026741300020>
- [14] Choi S., Kim J.: Thermal conductivity of epoxy composites with a binary-particle system of aluminum oxide and aluminum nitride fillers. *Composites Part B: Engineering*, **51**, 140–147 (2013).
<https://doi.org/10.1016/j.compositesb.2013.03.002>
- [15] Chen C., Xue Y., Li X., Wen Y., Liu J., Xue Z., Shi D., Zhou X., Xie X., Mai Y-W.: High-performance epoxy/binary spherical alumina composite as underfill material for electronic packaging. *Composites Part A: Applied Science and Manufacturing*, **118**, 67–74 (2019).
<https://doi.org/10.1016/j.compositesa.2018.12.019>
- [16] Ouyang Y., Ding F., Bai L., Li X., Hou G., Fan J., Yuan F.: Design of network Al₂O₃ spheres for significantly enhanced thermal conductivity of polymer composites. *Composites Part A: Applied Science and Manufacturing*, **128**, 105673 (2020).
<https://doi.org/10.1016/j.compositesa.2019.105673>
- [17] Wang H., Li L., Wei X., Hou X., Li M., Wu X., Lin C-T., Jiang N., Yu J.: Combining alumina particles with three-dimensional alumina foam for high thermally conductive epoxy composites. *ACS Applied Polymer Materials*, **3**, 216–225 (2020).
<https://doi.org/10.1021/acsapm.0c01055>
- [18] Yang S., Huang Z., Hu Q., Zhang Y., Wang F., Wang H., Su Y.: Proportional optimization model of multi-scale spherical BN for enhancing thermal conductivity. *ACS Applied Electronic Materials*, **4**, 4659–4667 (2022).
<https://doi.org/10.1021/acsaelm.2c00878>
- [19] Zhou X., Zong J., Lei J., Li Z.: Enhancing thermal conductivity of silicone rubber via constructing hybrid spherical boron nitride thermal network. *Journal of Applied Polymer Science*, **139**, 51943 (2022).
<https://doi.org/10.1002/app.51943>
- [20] Li D., Zeng D., Chen Q., Wei M., Song L., Xiao C., Pan D.: Effect of different size complex fillers on thermal conductivity of PA6 thermal composites. *Plastics, Rubber and Composites*, **48**, 347–355 (2019).
<https://doi.org/10.1080/14658011.2019.1626596>
- [21] Zheng Z., Xu H., Wen J., Chen J., Mao Z., Zhu P., Sun R., Wu W., Peng J.: *In-situ* growth of diamond/Ag as hybrid filler for enhancing thermal conductivity of liquid crystal epoxy. *Diamond and Related Materials*, **141**, 110659 (2024).
<https://doi.org/10.1016/j.diamond.2023.110659>
- [22] Kumlutas D., Tavman I. H.: A numerical and experimental study on thermal conductivity of particle filled polymer composites. *Journal of Thermoplastic Composite Materials*, **19**, 441–455 (2006).
<https://doi.org/10.1177/0892705706062203>

- [23] Agrawal A., Satapathy A.: Mathematical model for evaluating effective thermal conductivity of polymer composites with hybrid fillers. *International Journal of Thermal Sciences*, **89**, 203–209 (2015).
<https://doi.org/10.1016/j.ijthermalsci.2014.11.006>
- [24] Lewis T. B., Nielsen L. E.: Dynamic mechanical properties of particulate-filled composites. *Journal of Applied Polymer Science*, **14**, 1449–1471 (1970).
<https://doi.org/10.1002/app.1970.070140604>
- [25] Ngo I-L., Byon C.: A generalized correlation for predicting the thermal conductivity of composites with heterogeneous nanofillers. *International Journal of Heat and Mass Transfer*, **90**, 894–899 (2015).
<https://doi.org/10.1016/j.ijheatmasstransfer.2015.06.069>
- [26] Hashin Z., Shtrikman S.: A variational approach to the theory of the effective magnetic permeability of multiphase materials. *Journal of Applied Physics*, **33**, 3125–3131 (1962).
<https://doi.org/10.1063/1.1728579>
- [27] Meng T., Peng C., Wang R., Feng Y.: Effective thermal conductivity of ellipsoidal inclusion-reinforced composites: Data-driven prediction. *International Communications in Heat and Mass Transfer*, **152**, 107296 (2024).
<https://doi.org/10.1016/j.icheatmasstransfer.2024.107296>
- [28] Wang X., Niu X., Wang X., Qiu X., Wang L.: Effects of filler distribution and interface thermal resistance on the thermal conductivity of composites filling with complex shaped fillers. *International Journal of Thermal Sciences*, **160**, 106678 (2021).
<https://doi.org/10.1016/j.ijthermalsci.2020.106678>
- [29] Wang X., Gu W., Lu H.: A new thermal conductivity relational expression for polymer composites with con-structural design fillers. *International Communications in Heat and Mass Transfer*, **136**, 106198 (2022).
<https://doi.org/10.1016/j.icheatmasstransfer.2022.106198>
- [30] Ngo I-L., Byon C.: A novel correlation for predicting the thermal conductivity of heterogeneous nanofiller polymer composites under effects of thermal contact resistance. *International Journal of Heat and Mass Transfer*, **106**, 539–545 (2017).
<https://doi.org/10.1016/j.ijheatmasstransfer.2016.09.003>
- [31] Tsekmes I. A., Kochetov R., Morshuis P. H. F., Smit J. J.: Modeling the thermal conductivity of polymeric composites based on experimental observations. *IEEE Transactions on Dielectrics and Electrical Insulation*, **21**, 412–423 (2014).
<https://doi.org/10.1109/TDEI.2013.004142>
- [32] Zhao J-W., Zhao R., Huo Y-K., Chen W-L.: Effects of surface roughness, temperature and pressure on interface thermal resistance of thermal interface materials. *International Journal of Heat and Mass Transfer*, **140**, 705–716 (2019).
<https://doi.org/10.1016/j.ijheatmasstransfer.2019.06.045>
- [33] Wang C., Lin Q., Pan Z., Hong J., Shao H., Mai Y. W.: Optimization design method of material stiffness of contact interface considering surface roughness for improving thermal contact performance. *International Communications in Heat and Mass Transfer*, **149**, 107131 (2023).
<https://doi.org/10.1016/j.icheatmasstransfer.2023.107131>